Estimating the Shielding Failure Flashover Rate of Single-Circuit Overhead Lines with Horizontal Phase Configuration via Stochastic Lightning Attachment Simulations

A. I. Ioannidis, Z. G. Datsios, T. E. Tsovilis

***Abstract*—A methodology is proposed for estimating the shielding failure flashover rate (*SFFOR*) of single-circuit overhead lines with horizontal phase configuration. An application to a 66 kV overhead line is presented. A stochastic lightning attachment model is employed, based on the concept of fractal structures, to compute the probability of shielding failure to the line. Results of stochastic modeling are combined with those of an ATP-EMTP model for estimating the critical lightning currents causing flashover of the line insulation. Shielding failure results of the proposed methodology are compared and discussed with results obtained employing the methodology of the IEEE Std 1243. Innovation of this work lies in estimating the *SFFOR* of overhead lines by considering the stochastic nature of lightning attachment, physical criteria associated with leader discharges' inception and propagation, as well as electromagnetic transient simulations to predict lightning-related flashover to overhead lines accurately.**

***Keywords*: ATP-EMTP, lightning attachment, shielding failure flashover, stochastic modeling, overhead transmission lines.**

I. Introduction

Lightning is one of the main causes of unscheduled power supply interruptions in overhead power lines (OHLs), which comprise a major component of the power network. Thus, it significantly affects the reliability and continuous operation of the power supply [1], [2].

In this respect, OHLs are shielded against direct lightning strikes with the aid of shield wire(s). These wires aim to intercept the lightning downward leader through a connecting upward discharge. Nevertheless, lightning strikes, which are usually associated with low-intensity currents may still not be intercepted by the shield wires and strike the phase conductors (shielding failures). This causes flashover of line insulation when the arising fast-front overvoltages are higher than the insulation level of the line. Thus, the analysis of shielding failures and the estimation of the shielding failure flashover rate, *SFFOR*, of OHLs, that is, the annual number of insulation flashovers per 100 km of the line due to shielding failures, still attracts wide attention from the scientific community [3]-[9] as it results in significant economic losses [10], [11]. For instance, shielding failures are the main cause of power outages in UHV OHLs in Japan and lightning outages caused by shielding failures may reach up to 92% for 500 kV OHLs in China [12].

The estimation of lightning incidence to OHLs requires the use of a lightning attachment model, an engineering model comprising analytical formulas or employing computer simulations, to compute the annual number of direct lightning strikes to the OHL and dictate the positioning of shield wire(s) to provide perfect shielding to the OHL. These models can be generally categorized in the so called electrogeometric models (EGM) [13], [14] and leader propagation models (LPM) [15], [16] also adopted by the relevant international standards [17], [18]. More recently, computer-based physical models and models of lightning attachment employing fractal structures have been proposed [19]-[22]. In addition, electromagnetic transient (EMT) simulations [23]-[25] can be performed to calculate the minimum shielding failure current causing flashover of line insulation, assisting in shielding design analysis [26], [27].

This work introduces a methodology for estimating the *SFFOR* of single-circuit OHLs with horizontal phase configuration by combining stochastic lightning attachment simulations with EMT simulations. The proposed methodology is applied to a 66 kV OHL. The use of a stochastic model, based on the concept of fractal structures and adopting physical criteria for leader inception and propagation, allows for the estimation of the probability of shielding failure to the line, as well as the distribution of shielding failures along the span; thus, the most exposed parts of the line can be determined. The critical currents causing flashover of the 66 kV line insulation were estimated via ATP-EMTP [28], [29] simulations, employing accurate modeling of each line component. Results of the two models were combined to compute the *SFFOR* of the 66 kV line, which was then compared with *SFFOR* results computed through the methodology suggested by the IEEE Std 1243 [17].

The proposed methodology can be applied using any lightning attachment model which yields stochastic results, combined with an EMT simulation model. Thus, this study is a step towards the formation of a generalized approach for the assessment of the lightning performance of OHLs, including the estimation of their backflashover rate, *BFR*.

The research project was supported by the Hellenic Foundation for Research and Innovation (H.F.R.I.) under the "2nd Call for H.F.R.I. Research Projects to support Post-Doctoral Researchers" (Project Number: 367)

A. I. Ioannidis, Z. G. Datsios, and T. E. Tsovilis are with the High Voltage Laboratory, School of Electrical & Computer Engineering, Aristotle University of Thessaloniki, Thessaloniki, 541 24 Greece (e-mail of corresponding author: ialexios@ece.auth.gr, e-mails: zdatsios@auth.gr, tsovilis@auth.gr).

Paper submitted to the International Conference on Power Systems Transients (IPST2023) in Thessaloniki, Greece, June 12-15, 2023.

II. Shielding Failure Flashover Rate Estimation Methodology

This section presents the proposed methodology for estimating the shielding failure flashover rate, *SFFOR*, of single-circuit OHLs with horizontal phase configuration based on a stochastic modeling approach for lightning attachment. The latter occurs through a connecting positive upward leader intercepting the leader descending from the cloud. The upward leader emerges from a conductor (shield wire or phase conductor) due to the local electric field enhancement caused by the approaching downward leader.

According to the classical EGM analysis (Fig. 1), the rate of lightning strikes to phase conductors of an OHL, called shielding failure rate, *SFR* (flashes/100 km/yr), can be expressed as [17]:

$$SFR = 0.2 N_G \cdot \int_0^{I_{\mathrm{MSF}}} W(I)\, f(I)\, dI \tag{1}$$

where:

- N_G (flashes/km^2/yr) is the ground flash density along the OHL,
- I_{MSF} (kA) is the maximum shielding failure current, defined as the maximum lightning peak current that may terminate to phase conductors (Fig. 1),
- W (m) is the shielding failure width, defined as the lateral width along the OHL within which the downward leader may strike phase conductors (Fig. 1), and
- $f(I)$ is the probability density function of the lightning peak current distribution given as [30]:

$$f(I) = \frac{1}{\sqrt{2\pi}\sigma_{\ln} I} \exp\left[-\frac{(\ln I - \ln \bar{I})^2}{2\sigma_{\ln}^{\,2}} \right] \tag{2}$$

where $\bar{I}$ and $\sigma_{\ln}$ are, respectively, the median value and the standard deviation of the natural logarithm of the lightning peak current distribution.

Thus, the shielding failure flashover rate, *SFFOR* (flashovers/100 km/yr), which is the rate of lightning strikes to phase conductors resulting in insulation flashover, is [17]:

$$SFFOR = 0.2 N_G \cdot \int_{I_c}^{I_{\mathrm{MSF}}} W(I)\, f(I)\, dI \tag{3}$$

where I_c (kA) is the minimum shielding failure current causing flashover of line insulation computed using simplified expressions [17], [26], [31], [32] or more accurately with the aid of EMT simulations [26].

According to the proposed stochastic approach the rate of direct lightning strikes to phase conductors of a single-circuit OHL, *SFR* (flashes/100 km/yr) and the shielding failure flashover rate, *SFFOR* (flashovers/100 km/yr) caused by direct lightning strikes to phase conductors can be calculated as:

$$SFR = \frac{\sum_{i=1}^{N} SFR_i}{N} \tag{4a}$$

$$SFFOR = \frac{\sum_{i=1}^{N} SFFOR_i}{N} \tag{4b}$$

where N is the number of the phase angles of the AC operating voltage of the OHL considered and SFR_i, $SFFOR_i$ are the *SFR* and *SFFOR* for each phase angle, respectively computed as:

$$SFR_i = 0.1 \cdot N_G \int_0^{\infty} \left[2R(I) + b \right] \cdot p_{SFi}(I) \cdot f(I)\, dI \tag{5a}$$

$$SFFOR_i = 0.1 \cdot N_G \int_{I_{ci}}^{\infty} \left[2R(I) + b \right] \cdot p_{SFi}(I) \cdot f(I)\, dI \tag{5b}$$

where p_{SFi} is the probability of shielding failure to the OHL, defined as the number of lightning strikes to phase conductors versus the total number of direct lightning strikes to the OHL (at AC voltage phase angle i), R is the interception radius of the shield wire, defined as the maximum lateral distance between the interception point of downward and upward connecting leader and the shield wire of the OHL (inset of Fig. 1), and b (m) is the separation distance between the shield wires. In this study, 12 phase angles (30° increments) were considered corresponding to the maximum, minimum, and zero crossings of each phase (Fig. 2). It should be noted that (4b) and (5b) have been derived for symmetric OHLs of horizontal phase configuration (phase conductors on the same height above earth). This is due to the fact that in this case, the minimum shielding failure flashover currents are practically equal among phase conductors for the same AC voltage; thus, in (5b) a p_{SFi} can be considered for the OHL, without distinguishing between p_{SFi} values per phase conductor. In the general case of different OHL configurations, such as that of vertical conductor alignment, I_{ci} may differ among phase conductors for the same AC voltage and hence, p_{SFi} shall be considered separately for each of them.

Based on the stochastic approach, the downward leader may enter the region of lightning strikes to the shield wire (blue curves in Fig. 1) but still strike the phase conductor; this is because in the proposed approach the lightning branching and tortuosity are considered in contrast with the purely deterministic approach of the classical EGM analysis (propagation in a straight line, Fig. 1). In this work, *R(I)* and $p_{SF}(I)$ values are obtained from a stochastic lightning attachment model based on the concept of fractal structures (Section III) and I_{ci} is computed via ATP-EMTP simulations (Section IV). However, it should be emphasized that the proposed methodology is applicable to any stochastic approach for lightning attachment and EMT modeling technique. Expressions (4) and (5), based on a stochastic approach, are proposed as alternatives of (1) and (3) of IEEE Std 1243 [17], aiming at a more accurate *SFFOR* estimation on a physical basis. The latter can be accomplished, as shown in the application to the 66 kV OHL presented in what follows, by combining critical shielding failure flashover current estimation via detailed ATP-EMTP simulations with lightning incidence results obtained through a fractal-based model; this model considers the stochastic nature of lightning attachment phenomenon and physical parameters derived from lightning discharge physics/ field observations. Thus, simplifications on *SFFOR* estimation based on the IEEE Std 1243 procedures could be remedied.

Accurate estimation of the *SFFOR* requires knowledge of the lightning activity along the OHL. In this study, lightning strikes of negative polarity were considered for simulations and calculations as it typically accounts for the majority of lightning events [30]. Nevertheless, the proposed methodology [(4) and (5)] can also be applied for positive lightning; this is important when an OHL is located in a region exhibiting a high percentage of positive lightning that may significantly affect *SFFOR*.

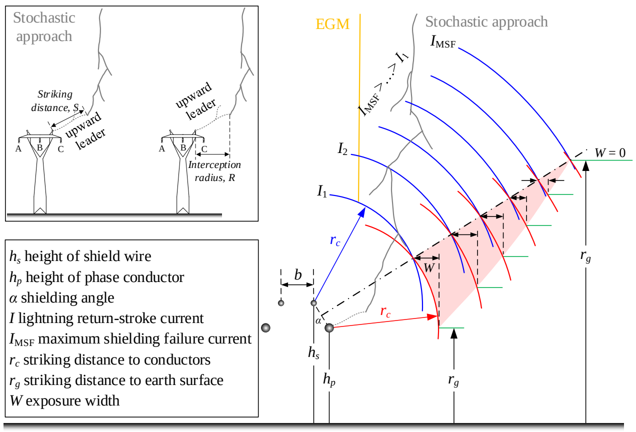

Fig. 1. Lightning attachment to OHLs according to the classical electrogeometric analysis and stochastic approach; adapted from [2].

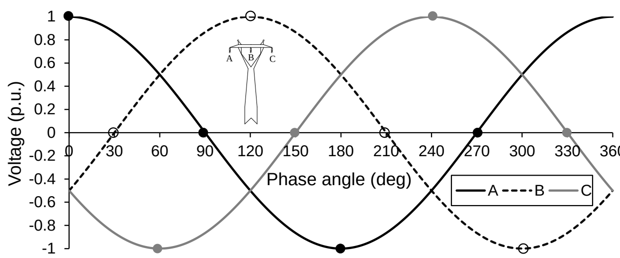

Fig. 2. AC cosine voltage function; dots designate the phase angles considered in this work (total number N = 12, 30° increments).

III. Stochastic Modeling of Lightning Incidence to Overhead Lines

In this section, the basic elements of the stochastic lightning attachment model used for lightning incidence simulations are presented. Section III.A deals with the main algorithm steps. OHL modeling technique is presented in Section III.B. Stochastic model results, which will be further used for the estimation of the *SFFOR* of the 66 kV OHL (Section V), are presented in Section III.C.

A. Model Description

Lightning discharge is a natural phenomenon characterized by intensive branched and tortuous features; these can be easily observed in both dedicated field measurements [33] and naked-eye observations. A stochastic lightning attachment model was developed and employed in this study to reproduce lightning discharges (quantitatively and qualitatively) as fractal structures and their main characteristic of self-similarity [34]. In this way, lightning incidence to OHLs can be simulated considering the randomness of the lightning attachment phenomenon. The simulation domain and OHL configuration were modeled in MATLAB software environment employing a uniform grid spacing. The model simulates the propagation of the downward stepped leader emanating from the cloud surface and progressing in a stepwise manner towards the ground, as well as the inception and consequent propagation of multiple upward leaders from the OHL under study up to the attachment phase. Physical parameters are employed based on lightning discharge physics and field measurements/ observations to account for a more accurate representation of the lightning attachment phenomenon [7], [34], [35]. The basic algorithm steps are presented in Fig. 3.

B. 66 kV OHL Modeling

Modeling of the 66 kV OHL is performed considering the geometry and dimensions of transmission towers, as well as phase conductor and shield wire type and characteristics to account for the sag along the OHL span; two spans of 250 m were integrated into the model. The tower and span geometry were adapted to the defined grid spacing utilized for discretizing the 3D simulation domain (Fig. 3) and to the employed Cartesian coordinates system; thus, approximations on tower modeling were adopted, as well as a staircase approximation for the OHL conductors. Phase conductor and shield wire sags have been modeled based on the catenary equation [36]. The 66 kV OHL tower and span geometry are depicted in Fig. 4; two tower geometries were adopted corresponding to a tension (tower type A) and suspension tower (tower type B) to study the differences between the adopted geometries on *SFFOR* values. OHL's characteristics are listed in the inset table of Fig. 4. Lightning incidence results only between midspan-to-midspan were considered (Fig. 4), as segments close to the lateral towers are strongly affected by the lateral simulation boundaries and are not representative.

OHL is modeled as points of fixed electric potential imposed as initial boundary conditions in the algorithm at each simulation step. Thus, the power frequency voltage of phase conductors is considered in simulations to accurately represent the actual case of energized OHLs, as in the field, and investigate the possible effect of the power frequency voltage

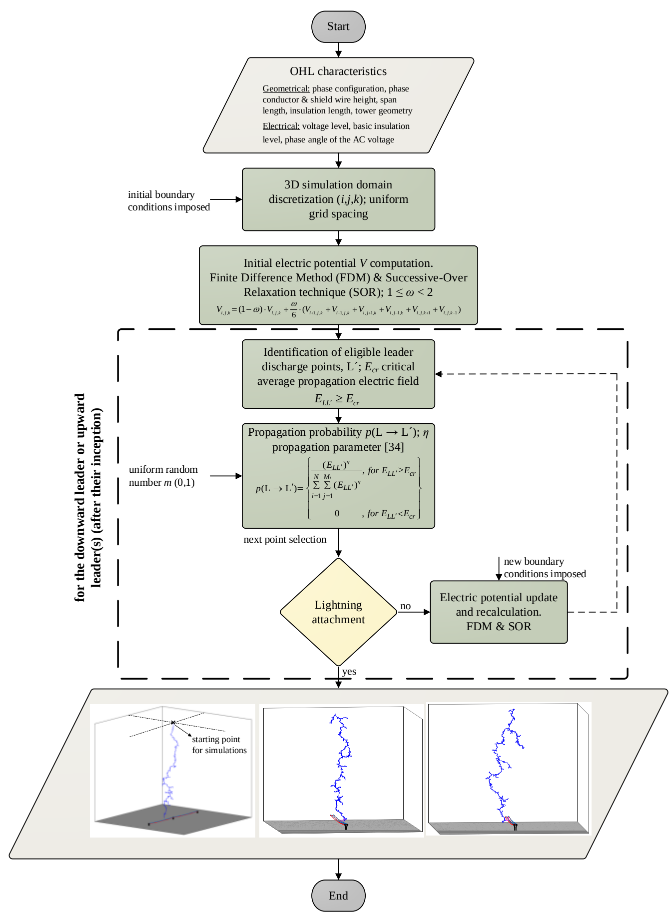

Fig. 3. Flowchart of the employed stochastic lightning attachment model for estimating lightning incidence to OHLs.

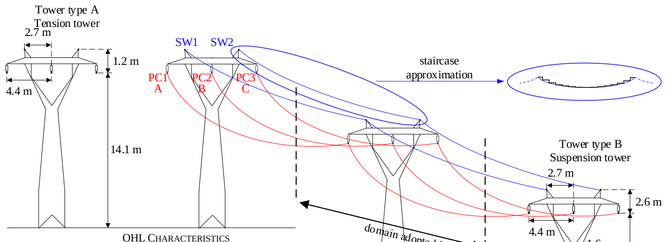

OHL CHARACTERISTICS

Operating voltage	Span length	Conductor	Conductor sag
66 kV	250 m	1 x ACSR Raccoon	4 m
Phase conductor diameter	Shield wire type	Shield wire sag	Shield wire diameter
12.30 mm	2x Glv Steel	3 m	6.16 mm
Insulator string length	*BIL*	Shielding angle at tower type A	Shielding angle at tower type B
0.73 m	325 kV	54.8°	34°

Fig. 4. Transmission tower geometries (not according to scale) and overhead line configuration for the 66 kV single-circuit OHL under examination; the staircase approximation is also demonstrated. OHL's characteristics are listed in the inset table; the considered simulation part (midspan-to-midspan) is depicted between dashed lines.

on lightning incidence. A constant electric potential was used for phase conductors as the lightning attachment phenomenon is very short in duration compared to the variation of the operating voltage. The simulated scenarios regarding the AC voltage phase angle are presented in the following subsection.

Finally, with respect to the upward leader inception points, the proposed stochastic lightning attachment model simulates upward leader propagation from different points of the OHL. Specific inception points were selected along the OHL span to avoid huge computational times associated with upward leader inception from every possible point of the geometry. More specifically, points at the tower crossarm and body were chosen to allow for classical lightning incidence scenarios and lateral hits, as well as points along the shield wire and phase conductor span. The latter were selected at every 25 m along the span, as lower critical point separation distances did not affect the lightning strike distribution along the span.

C. *Interception Radius and Shielding Failure Probability*

Simulations were performed at the High-Performance Computing Infrastructure (HPC) of the Aristotle University of Thessaloniki. Lightning peak currents in the range of 5-50 kA and 12 AC voltage phase angles (30° increments, Fig. 2) were investigated. One thousand simulation runs were conducted at each lightning peak current level for each phase angle to obtain a sufficient statistical sample of stochastic model results. As this work focuses on the analysis of the shielding failure flashover characteristics of the 66 kV OHL and its *SFFOR*, the adequate number of simulation runs (1000) was obtained employing a stopping criterion for the simulations when p_{SF} to the OHL converges to a value that results in changes on the computed $SFFOR \leq 5\%$. It should be noted that every simulation yields a different lightning termination scenario to the OHL due to the propagation probability distribution and random number generator used (Fig. 3). Indicative simulation results of the stochastic model regarding lightning incidence to the 66 kV OHL are presented in Fig. 3.

Fig. 5 shows results obtained through the stochastic model for basic shielding design parameters i.e., the interception radius R (Fig. 5a) and striking distance S (Fig. 5b). As R and S for the two tower geometries were found to vary slightly, results for tower type B are only shown in Fig. 5. In Fig. 5a, interception radius results based on the stochastic model are compared with the commonly employed models of A. J. Eriksson [14], F. A. M. Rizk [15], and Petrov *et al.* [37], as well as the EGM by IEEE Std 1243 [17]; a very good agreement exists between stochastic model results and Rizk's model [15]. In addition, stochastic model results lie between the values obtained by the IEEE Std 1243 [17] and Eriksson's [14] model (Fig. 5). It is important that the employed lightning attachment models from literature refer to average conductor height and do not consider the AC voltage of the line. Nevertheless, when considering the latter by employing the stochastic model, no significant deviation was found for $R(I)$; this could be due to the relatively low operating voltage of the 66 kV OHL under study. Fig. 5b shows striking distance values based on stochastic modeling, the EGM of the IEEE Std 1243 [17], fractal-based models from literature [21], [38], [39], and field data from Miki et al. [40]. The statistical dispersion of the stochastic model striking distance is in satisfactory agreement with the field observations [40] and predicts reasonable values with respect to the fractal-based models [21], [38], [39] when considering that the latter refer to different configurations.

Fig. 6 depicts the probability of shielding failure, p_{SF}, to the 66 kV OHL for 3 AC voltage phase angles (30°, 150°, and 270°). These correspond to the zero-crossings of the AC voltage for negative-to-positive transition (Fig. 2). It can be observed that (i) tower A exhibits higher p_{SF} values than tower B due to its significantly larger shielding angle and (ii) p_{SF} for all phase angles attains similar values denoting no significant effect of the AC voltage variation; this is attributed to the relatively low voltage of the 66 kV OHL. A slight increase in

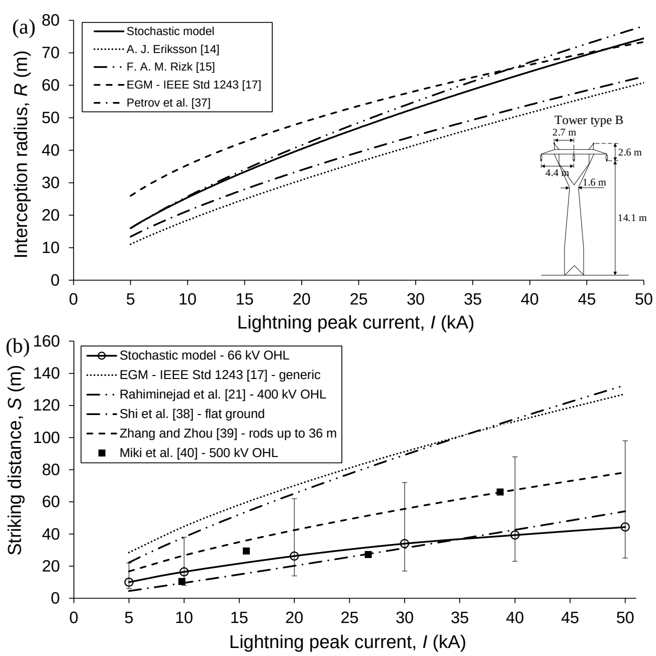

Fig. 5. (a) Interception radius, R, of the shield wire of the 66 kV OHL (Figs. 1 and 4) obtained by stochastic modeling and commonly adopted models from literature; results of the latter refer to average height. (b) Striking distance of the shield wire of the 66 kV OHL (Figs. 1 and 4) obtained via stochastic modeling, fractal-based models from literature [21], [38], [39], the EGM by IEEE Std 1243 [17], and field data from Miki et al. [40].

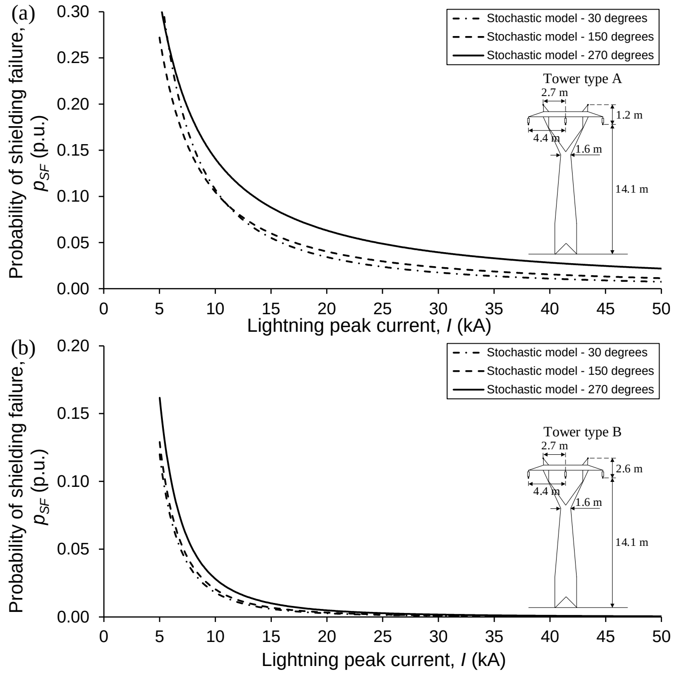

Fig. 6. Probability of shielding failure to the 66 kV single-circuit OHL for three phase angles (30°, 150°, and 270°) of the AC cosine voltage function (Fig. 2). (a) Tower type A and (b) tower type B.

p_{SF} values can be seen in Fig. 6 for 270°; the same was found for 300° and 330°. This can be attributed to the fact that the AC voltage of both outer phase conductors is ≥ 0 kV at these phase angles (Fig. 2), that is, the polarity of the AC voltage of the more exposed phase conductors is opposite to that of lightning. Hence, the probability of upward leader inception from the outer phase conductors at these phase angles is higher. Nevertheless, these differences are small considering the low operating voltage of the 66 kV OHL and are expected to be more significant for OHLs of higher voltage levels (such as EHV and UHV lines) where upward leader inception and propagation is of greater importance.

IV. EMT Modeling and Simulations

This section describes the EMT simulation model of the 66 kV OHL used to estimate the minimum (critical) lightning currents causing flashover of line insulation for direct lightning strikes to phase conductors. It also presents the computed critical currents for the 12 AC voltage phase angle values shown in Fig. 2. These critical currents will be used for the estimation of the *SFFOR* of the 66 kV OHL in Section V. It should be noted that the effect of the two tower geometries (Fig. 4) on critical current estimation employing the developed EMT model was found negligible; thus, in the following, results refer to both tower geometries (Fig. 4).

A. Model Description

The EMT simulation model of the 66 kV OHL was developed in ATP-EMTP [28], [29] software by adapting the modeling technique of [41]-[43] considering line geometry and basic characteristics (Fig. 4). The model was used to compute the overvoltages stressing line insulators due to direct lightning strikes to phase conductors and to predict insulator flashover due to these non-standard fast-front overvoltages. Thus, the critical shielding failure flashover currents can be determined.

For simulations of lightning strikes to phase conductors, the representation of the OHL conductors, the lightning return-stroke (equivalent channel impedance and waveform), and the model used for insulation flashover prediction are of crucial importance. The AC operating voltage should also be considered as overvoltages due to shielding failure are superimposed on the instantaneous AC voltage value. In this study, the OHL was represented by a JMarti [44] frequency-dependent model for each span (soil resistivity for line parameter calculation: 100 Ωm). The CIGRE lightning current waveform [31], [32] was used (waveshape parameters: median values) with a 1000 Ω lightning channel impedance [42]. The CIGRE leader development model [31] was adopted for insulator flashover prediction (parameters: cap-and-pin insulators, negative polarity).

B. Model Results

Fig. 7a shows lightning overvoltages stressing the nearest insulator to the lightning strike position for a shielding failure at the outer phase A. Three phase angles of the AC voltage were considered corresponding to positive (0°) and negative (180°) peak values of the AC voltage, as well as zero AC voltage (90°). The applied lightning current is 2 kA (selected lower than the critical value). It is evident that the lightning overvoltage is non-standard. It is superimposed on the AC voltage of the line at the instant of lightning strike. Fig. 7b shows the lightning overvoltages corresponding to critical flashover for these three AC voltage phase angles. It can be seen that the instantaneous flashover voltage and time differ among phase angle values. However, the peak overvoltage values are almost equal. The lowest critical current was found for the 180° as this phase angle yields the negative AC voltage peak facilitating flashover due to higher overvoltages (Fig. 7a).

Fig. 8 shows the variation of the critical shielding failure flashover current, I_{ci}, of the 66 kV OHL with the phase angle of the AC voltage (Fig. 2) for phases A (outer), B (middle), and C (outer). It is evident that the highest value is ~32% higher than the threshold value of 2.05 kA. The latter is so low due to the low Basic Insulation Level, *BIL*, of the line (Fig. 4, 325 kV). Such low I_c values indicate that all lightning strikes to phase conductors would yield flashover and, thus, *SFR* = *SFFOR* for the 66 kV OHL under study.

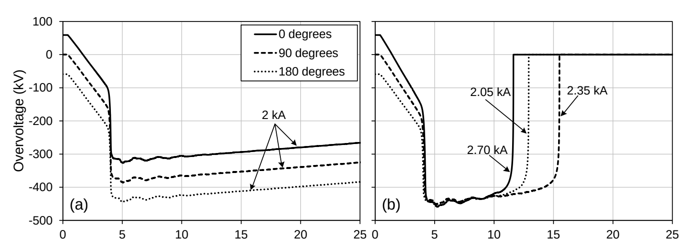

Fig. 7. Overvoltages due to shielding failure at the outer phase A of the 66 kV OHL (Fig. 4) across the nearest insulator to the lightning strike position. (a) Withstand case and (b) critical shielding failure flashover. AC voltage phase angles: 0°, 90°, 180°.

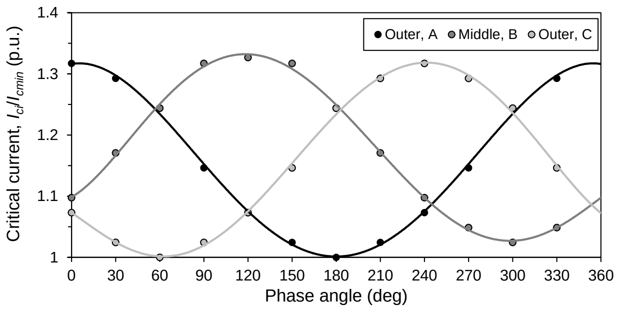

Fig. 8. Variation of the critical shielding failure flashover current, I_{ci}, of the 66 kV OHL (Fig. 4) with the phase angle of the AC voltage (Fig. 2). Results normalized to the threshold (minimum) I_{ci} value (2.05 kA).

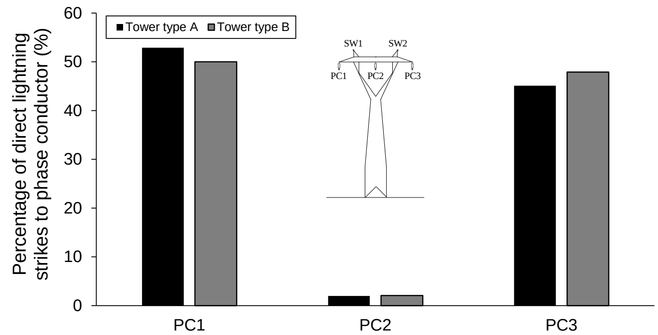

Fig. 9. Percentage of direct lightning strikes to the phase conductors of the 66 kV OHL, defined as the number of lightning strikes to each phase conductor versus the total number of shielding failures to the OHL.

V. Results and Discussion on Shielding Failure Distribution and *SFFOR*

This section presents results on the distribution of shielding failures to the 66 kV OHL and on *SFFOR* obtained by combining stochastic lightning attachment and EMT simulations (Sections III and IV). Fig. 9 depicts the percentage of direct lightning strikes to each phase conductor of the investigated 66 kV OHL (Fig. 4) for all the examined phase angles of the AC voltage of the line and the two tower geometries. It is important that a clear effect of the AC voltage variation was not determined, possibly due to the relatively low operating voltage of the 66 kV OHL; thus, results for all phase angles were merged. As seen from Fig. 9, the distribution of direct lightning strikes to the outer phases of the OHL is almost equal due to its symmetric configuration and this difference is expected to fade away for a significantly larger number of simulations. The middle phase experiences the least number of direct lightning strikes as it is shielded not only by the two shield wires but also by the other two phase conductors (inset in Fig. 9). It is important that traditional lightning attachment models (such as EGMs) are deterministic and cannot predict shielding failures for the middle phase conductor in case of single-circuit OHLs of horizontal phase configuration.

Fig. 10 shows the distribution of direct lightning strikes along the span for the phase conductors of the 66 kV OHL for all considered AC voltage phase angles and the two tower geometries; thus, the most exposed parts of the OHL can be determined. Results for the outer phases (Figs. 10a and 10c) were merged due to symmetry; the middle phase was treated separately (Figs. 10b and 10d) indicating "weak" points.

From Figs. 10a and 10c it can be observed that the percentage of shielding failures to the outer phases vary non-monotonically along the span from tower to midspan being highest close to the tower (segments 10 and 12). Differences in the percentage of shielding failures for segments 6-10 and 16-12 are expected to fade away for a significantly larger number of simulations due to the symmetry of the 66 kV OHL. In addition, the highest percentage of shielding failure cases in segments closer to tower location (segments 10 and 12) as compared with tower location (segment 11) may be ascribed to the shielding effect provided by the tower structure at segment 11. Shielding failure analysis close to the lateral towers (towers #1 and #3) was not considered representative due to their close proximity to the lateral simulation boundaries.

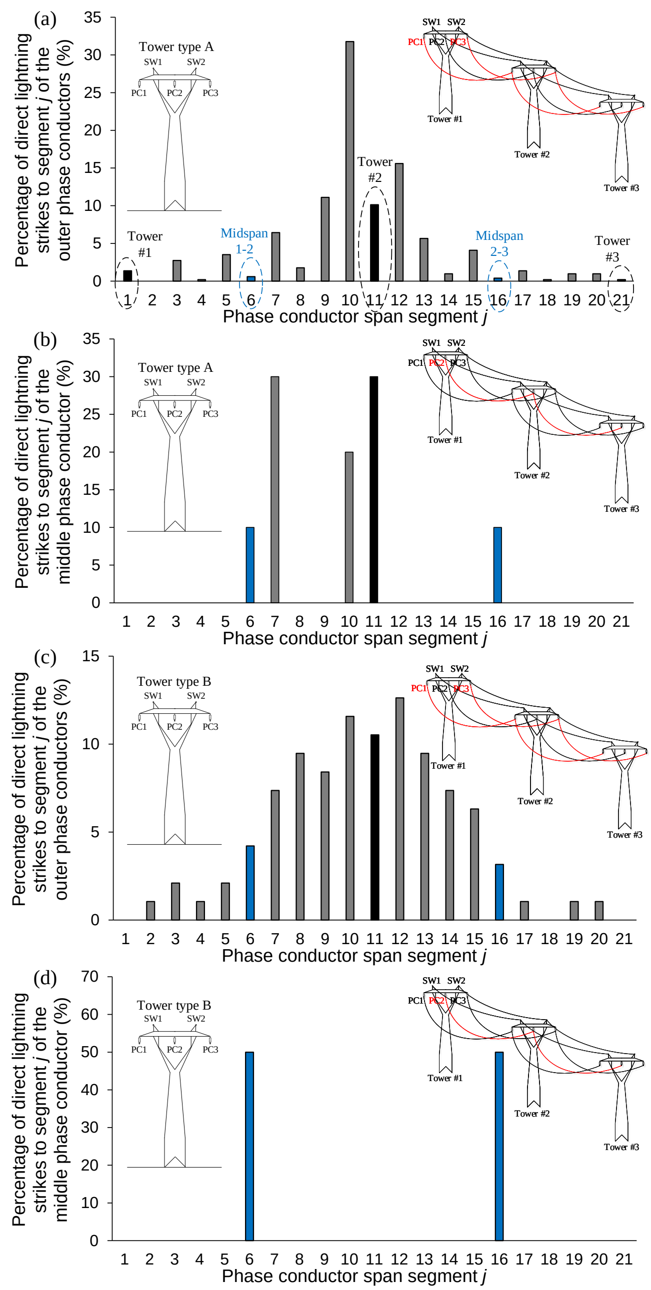

Fig. 10. Percentage of direct lightning strikes along the phase conductor span of the 66 kV OHL, defined as the number of direct lightning strikes at each segment j along the span versus the total number of shielding failures to the (a) & (c) outer phase conductors of tower types A and B, respectively, and (b) & (d) middle phase conductor of tower types A and B, respectively.

Thus, results for segments in the range of 6-16 were only considered; the same applies also for results of Figs. 5 and 6. The rare shielding failure cases to the middle phase conductor shown in Figs. 10b and 10d are observed at the span segment at tower #2 and at midspan for tower type A and only at midspan location (segments 6 and 16) for tower type B.

It is important that the distribution of shielding failures along the span may be affected by (i) the operating AC voltage level, (ii) the OHL phase configuration, and (iii) the conductor sag values. These call for further investigations on OHLs of different voltage levels and configurations.

The critical lightning currents causing shielding failure flashover for all phase conductor insulators of the 66 kV OHL are ≤ 3 kA (Fig. 8). Hence, practically every shielding failure causes flashover and the *SFR* of the OHL is equal to the *SFFOR*. Thus, only *SFFOR* results are presented in Table I. These were computed by applying the methodology introduced in Section II [(4b) and (5b)] and the IEEE Std 1243 [17] methodology (3); the latter is applied for the heights at the tower location and for the average conductor height employing the EGM of the IEEE Std 1243 [17] and an EGM based on the striking distance expression derived from field data of Miki et al. [40] (Fig. 5b). Computations were performed for the CIGRE [30] lightning peak current distribution ($\bar{I}$ = 30 kA, $\sigma_{\ln}$ = 0.61) and a ground flash density N_G = 5 flashes/km^2/yr. Based on Table I results:

– the *SFFOR* computed by both the EGM methodology and the proposed stochastic approach is higher for tower type A associated with a larger shielding angle than tower type B.
– *SFFOR* results based on the EGM methodology depend notably on the adopted striking distance expression. In addition, they vary significantly depending on the adopted height for computations; as a compromise for long-term calculations, *SFFOR* results at the average line height are commonly considered so as to account for the shielding effect of the tower.
– *SFFOR* results based on the proposed stochastic approach can overcome simplifications of the EGM methodology, that suggests the use of (3) and average conductor height. This is because the adopted stochastic lightning attachment model considers the AC power frequency voltage variation, conductor sag, and exact line geometry in a 3D domain according to the formulated methodology of (4) and (5). Thus, the big discrepancies observed in *SFFOR* values (Table I) by the EGM methodologies for different conductor heights adopted can be remedied.

TABLE I
SFFOR RESULTS FOR THE 66 kV SINGLE-CIRCUIT OHL

Methodology	***SFFOR* (flashovers/100 km/yr) Tower type A[**]**	***SFFOR* (flashovers/100 km/yr) Tower type B[**]**
Proposed stochastic approach Equations (4) and (5)	1.932	0.1573
EGM of IEEE Std 1243 [17][*] Equation (3)	0.056 (5.101)	0.0007 (0.0232)
EGM based on data of Miki et al. [40][*] Equation (3)	1.203 (5.568)	0.2833 (0.7819)

[*] I_c calculated analytically based on [17]
[**] *SFFOR* values in parentheses refer to tower height

The proposed stochastic approach could integrate the effects of topology and terrain along the OHL as well as shielding effects from neighboring objects, which can lead to very complex computations employing the EGM. This is important for the accurate lightning performance assessment of practical line spans since they rarely extend along purely flat terrains.

VI. CONCLUSIONS

This work introduces a methodology for the estimation of the shielding failure flashover rate, *SFFOR*, of single-circuit overhead lines (OHLs) with horizontal phase configuration. The methodology is based on a stochastic approach for lightning attachment and electromagnetic transient simulations for determining the critical lightning currents causing line insulation flashover. It can be applied using any lightning attachment model which yields stochastic lightning incidence results, combined with an EMT simulation model.

An application to a 66 kV OHL is presented. A stochastic lightning attachment model, based on the concept of fractal structures, is adopted to estimate the probability of shielding failure to the line, the interception radius of the shield wires, as well as the distribution of shielding failures along the span. Results of the stochastic model are combined with ATP-EMTP simulations to calculate the minimum shielding failure flashover currents. It has been shown that:

– Shielding failures to the outer phase conductors of the 66 kV OHL comprise the vast majority and are almost equal for the two outer phases due to symmetry. The most are obtained close to the tower; a non-monotonic behavior has been observed along the span from tower to midspan.
– The middle phase conductor of the 66 kV OHL experiences the fewest direct lightning strikes. It is important that shielding failures at the middle phase cannot be predicted by the deterministic EGM analysis.
– The *SFFOR* of the 66 kV OHL computed by applying the proposed methodology lies in between the values obtained by the EGM methodology. *SFFOR* results employing the classical EGM analysis vary notably depending on the adopted striking distance expression and the height used for calculations.
– For the 66 kV OHL, the AC voltage variation has found not to affect the interception radius of the shield wires, the percentage of lightning strikes to each phase conductor, and the shielding failure distribution along the span. However, a slight increase in the shielding failure probability was observed when the polarity of the outer phases of the OHL was positive, that is, opposite to the negative lightning polarity considered in simulations. Application of the proposed methodology to OHLs of higher voltage levels and longer conductor sags may shed light on the effect of the AC voltage variation on the above parameters where upward leaders are of importance.

Finally, this study contributes to the formation of a generalized methodology for assessing the lightning performance of OHLs, including shielding failure flashover rate and backflashover rate estimation.

VII. ACKNOWLEDGMENT

Results presented in this work have been produced using the Aristotle University of Thessaloniki High-Performance Computing Infrastructure; the authors would like to acknowledge the support provided by Mr. P. Korosoglou, throughout the progress of this research work.

VIII. REFERENCES

[1] *Evaluation of lightning shielding analysis methods for EHV and UHV DC and AC transmission lines*, CIGRE Working Group C4.26, Technical Brochure 704, Oct. 2017.

[2] P. N. Mikropoulos, J. He, and M. Bernardi, "Lightning attachment to overhead power lines," in *Lightning Interaction with Power Systems - Volume 1: Fundamentals and Modelling*, Ed. A. Piantini: Institution of Engineering & Technology, Jan. 2020.

[3] P. N. Mikropoulos and T. E. Tsovilis, "Estimation of the shielding performance of overhead transmission lines: The effects of lightning attachment model and lightning crest current distribution," *IEEE Trans. Dielectr. Electr. Insul.*, vol. 19, no. 6, pp. 2155-2164, Dec. 2012.

[4] F. Napolitano, F. Tossani, A. Borghetti, and C. A. Nucci, "Lightning performance assessment of power distribution lines by means of stratified sampling Monte Carlo method," *IEEE Trans. Power Del.*, vol. 33, no. 5, pp. 2571-2577, Oct. 2018.

[5] B. Wei, Z. Fu, and H. Yuan, "Analysis of lightning shielding failure for 500-kV overhead transmission lines based on an improved leader progression model," *IEEE Trans. Power Del.*, vol. 24, no. 3, pp. 1433-1440, Jul. 2009.

[6] J. He, X. Wang, Z. Yu, and R. Zeng, "Statistical analysis on lightning performance of transmission lines in several regions of China," *IEEE Trans. Power Del.*, vol. 30, no. 3, pp. 1543-1551, Jun. 2015.

[7] Z. G. Datsios, A. I. Ioannidis, T. A. Papadopoulos, and T. E. Tsovilis, "A stochastic model for evaluating the lightning performance of a −400 kV HVDC overhead line," *IEEE Trans. Electromagn. Compat.*, vol. 63, no. 5, pp. 1433-1443, Oct. 2021.

[8] N. Malcolm and R. K. Aggarwal, "Assessment of shielding performance of 69/138 kV transmission lines exposed to lightning strikes," in *Proc. 2015 IEEE Power & Energy Society General Meeting*, pp. 1-5.

[9] A. Yamanaka and K. Ishimoto, "Revisiting the indirect lightning performance of distribution lines: Flashover analysis of typical Japanese lines by the Monte Carlo method," in *Proc. 2022 Int. Works. High Volt. Engin.*, pp. 37-42.

[10] M. Bruch, V. Münch, M. Aichinger, M. Kuhn, M. Weymann, and G. Schmid, "Power blackout risks: Risk management options," CRO Forum Emerging Risk Initiative, Amstelveen, The Netherlands, Nov. 2011.

[11] S. Ekisheva, M. Papic, M. G. Lauby, and M. Elkins, "Assessment of impact of AC circuit attributes to outage frequency in the WECC system," *IEEE Trans. Power Del.*, vol. 36, no. 2, pp. 1159-1172, Apr. 2021.

[12] A. Piantini, *Lightning Interaction with Transmission and Distribution Power Systems*, EMC Society Distinguished Lecturer Series, Apr. 2022.

[13] A. M. Mousa and K. D. Srivastava, "A revised electrogeometric model for the termination of lightning strokes on ground objects," in Proc. *1988 Int. Aeros. Ground Conf. Lightn. Stat. Electr.*, pp. 324-352.

[14] A. J. Eriksson, "An improved electrogeometric model for transmission line shielding analysis," *IEEE Trans. Power Del.*, vol. PWRD-2, no. 3, pp. 871-886, Jul. 1987.

[15] F. A. M. Rizk, "Modeling of transmission line exposure to direct lightning strokes," *IEEE Trans. Power Del.*, vol. 5, no. 4, pp. 1983-1997, Oct. 1990.

[16] L. Dellera, and E. Garbagnati, "Lightning stroke simulation by means of the leader progression model. I. Description of the model and evaluation of exposure of free-standing structures," *IEEE Trans. Power Del.*, vol. 5, no. 4, pp. 2009-2022, Oct. 1990.

[17] *IEEE Guide for Improving the Lightning Performance of Transmission Lines*, IEEE Std 1243, 1997.

[18] *IEEE Guide for Improving the Lightning Performance of Electric Power Overhead Distribution Lines*, IEEE Std 1410, 2010.

[19] M. Becerra and V. Cooray, "A simplified physical model to determine the lightning upward connecting leader inception," *IEEE Trans. Power Del.*, vol. 21, no. 2, pp. 897-908, Apr. 2006.

[20] A. Borghetti, F. Napolitano, C.A. Nucci, M. Paolone, and M. Bernardi, "Numerical solution of the leader progression model by means of the finite element method," in Proc. *2010 Int. Conf. Lightn. Prot.*, pp. 1-8.

[21] A. Rahiminejad, B. Vahidi, and J. He, "A fractal-based stepped downward leader model including branched channel charge distribution and branch fading," *Electr. Pow. Syst. Res.*, vol. 176, Nov. 2019.

[22] S. Xie, F. D'Alessandro, and X. Zhao, "A three-dimensional downward leader model incorporating geometric and physical characteristics," *Electr. Pow. Syst. Res.*, vol. 163, Part A, pp. 10-17, Oct. 2018.

[23] J. A. Martinez-Velasco (Ed.), *Power System Transients: Parameter Determination*, Boca Raton, FL, USA: CRC Press, 2010.

[24] A. Ametani, N. Nagaoka, Y. Baba, T. Ohno, and K. Yamabuki, *Power System Transients: Theory and Applications*, 2nd ed., Boca Raton, FL, USA: CRC Press, 2017.

[25] J. A. Martinez-Velasco (Ed.), *Transient Analysis of Power Systems – A Practical Approach*, Hoboken, NJ: John Wiley & Sons Ltd, 2020.

[26] Z. G. Datsios, P. N. Mikropoulos, and T. E. Tsovilis, "Estimation of the minimum shielding failure flashover current for first and subsequent lightning strokes to overhead transmission lines," *Electr. Pow. Syst. Res.*, vol. 113, pp. 141-150, Aug. 2014.

[27] Z. G. Datsios, A. I. Ioannidis, T. A. Papadopoulos, and T. E. Tsovilis, "A parametric study on the critical lightning currents causing flashover to the monopolar overhead lines of a ±533 kV HVDC transmission system," in *Proc. 2020 Int. Conf. Environ. Electr. Eng.*, pp. 1-6.

[28] Canadian-American EMTP Users Group, ATP Rule Book, 1997.

[29] H. W. Dommel, Electro-Magnetic Transients Program (EMTP) Theory Book. Portland, OR: Bonneville Power Administration, 1986.

[30] *Lightning parameters for engineering applications*, CIGRE Working Group C4.407, Technical Brochure 549, Aug. 2013.

[31] *Guide to procedures for estimating the lightning performance of transmission lines*, CIGRE Working Group 33.01, Technical Brochure 63, Oct. 1991.

[32] *Procedures for estimating the lightning performance of transmission lines – New aspects*, CIGRE Working Group C4.23, Technical Brochure 839, Jun. 2021.

[33] V. A. Rakov, M. D. Tran, Y. Zhu, Z. Ding, A. F. R. Leal, I. Kereszy, and S. Chen "New insights into the lightning discharge processes," *Plasma Sourc. Sci. Technol*., vol. 31, pp. 1-17, Nov. 2022, Art. no. 104005.

[34] A. I. Ioannidis, Z. G. Datsios, G. A. Tsaousakis, and T. E. Tsovilis, "Analysis of the fractal dimension of lightning discharges based on a stochastic lightning attachment simulation model," in Proc. *2022 Int. Conf. Lightn. Prot.*, pp. 1-6.

[35] A. I. Ioannidis and T. E. Tsovilis, "Shielding failure of high voltage substations: A fractal-based approach for negative and positive lightning," *IEEE Trans. Ind. Appl.*, vol. 57, no. 3, pp. 2317-2325, May-Jun. 2021.

[36] *Sag-tension calculation methods for overhead lines*, CIGRE Task Force B2.12.3, Technical Brochure 324, Apr. 2016.

[37] N. I. Petrov, G. Petrova, and R. T. Waters, "Determination of attractive area and collection volume of earthed structures," in *Proc. 2000 Int. Conf. Lightn. Prot.*, pp. 374-379.

[38] W. Shi, Q. Li, and L. Zhang, "A stepped leader model for lightning including charge distribution in branched channels," *J. Appl. Phys.*, vol. 116, no. 10, Sep. 2014, Article no. 103303.

[39] Q. Zhang, B. Zhou, "Identification of striking distance considering the velocity ratio and competition among the leaders," *J. Electrost.*, vol. 72, no. 5, pp. 365-371, Oct. 2014.

[40] M. Miki, T. Miki, D. Tanaka, T. Shindo, M. Hayashi, and M. Shimizu, "Observation of lightning flashes striking transmission lines using high-speed digital videos," Keynote speech *GROUND'2014 and 6th Int. Conf. Lightn. Phys. Effect*., Manaus, Brazil, May 2014.

[41] Z. G. Datsios, P. N. Mikropoulos, T. E. Tsovilis, and S. I. Angelakidou, "Estimation of the minimum backflashover current of overhead lines of the Hellenic transmission system through ATP-EMTP simulations," in *Proc. Int. Colloquium Lightn. Power Syst.*, CIGRE Study Committee C4, Bologna, Italy, Jun. 2016, paper no. 32.

[42] Z. G. Datsios, P. N. Mikropoulos, and T. E. Tsovilis, "Effects of lightning channel equivalent impedance on lightning performance of overhead transmission lines," *IEEE Trans. Electromagn. Compat.*, vol. 61, no. 3, pp. 623-630, Jun. 2019.

[43] Z. G. Datsios, P. N. Mikropoulos, and T. E. Tsovilis, "Closed-form expressions for the estimation of the minimum backflashover current of overhead transmission lines," *IEEE Trans. Power Del.*, vol. 36, no. 2, pp. 522-532, Apr. 2021.

[44] J. R. Marti, "Accurate modelling of frequency-dependent transmission lines in electromagnetic transient simulations," *IEEE Trans. Power App. Syst.*, vol. PAS-101, no. 1, pp. 147-157, Jan. 1982.